

# Design and Synthesis of Tetrahydropyrrolo[3,4-c]Pyrazole Sigma-1 Receptor Ligands

Giuseppe Cosentino,<sup>[a]</sup> Maria Dichiara,<sup>\*[a]</sup> Giuliana Costanzo,<sup>[a]</sup> Alessandro Coco,<sup>[a]</sup> Lorella Pasquinucci,<sup>[a]</sup> Agostino Marrazzo,<sup>[a]</sup> Antonio Rescifina,<sup>[a]</sup> and Emanuele Amata<sup>\*[a]</sup>

This study presents a series of tetrahydropyrrolo[3,4-c]pyrazole-based compounds designed as sigma-1 receptor (S1R) ligands, focusing on optimizing affinity and reducing off-target effects. We synthesized various derivatives from commercially available precursors and, through radioligand binding assays, assessed their binding affinity for S1R and sigma-2 receptor (S2R). Compound **19** (AD417), containing a benzyl group and an amide substituent, demonstrated notable S1R affinity ( $K_i = 75$  nM) with 6-fold selectivity over S2R. Modifications on the pyrrolidine nitrogen were crucial in enhancing receptor interaction, as the protonated nitrogen likely interacts with Glu172 within the S1R binding site. Furthermore, to address hERG

potassium ion channel inhibition, a known limitation in S1R drug development, we evaluated compound **19**'s cardiotoxicity potential. With an experimental hERG  $IC_{50}$  of 5.8  $\mu$ M, significantly higher than verapamil's  $IC_{50}$  of 0.41  $\mu$ M, and haloperidol's  $IC_{50}$  of 0.16  $\mu$ M, compound **19** showed a safer profile, suggesting a reduced risk of cardiotoxicity. These findings underscore the role of nitrogen accessibility, structural flexibility, and functional group modifications in optimizing S1R ligand interactions and provide a promising foundation for developing safer S1R-targeted therapeutics with minimized hERG-related risks.

## 1. Introduction

Sigma receptors (SRs) – initially misclassified as opioid receptors (ORs) – are unique, chaperone-like non-G protein-coupled receptors (GPCRs) with two subtypes: sigma-1 (S1R) and sigma-2 (S2R) receptors.<sup>[1]</sup> S1R is predominantly found within the endoplasmic reticulum (ER), especially in cholesterol-rich mitochondria-associated membranes (MAM). Structurally, it exists as a homotrimer, composed of three tightly associated protomers, with expression in both peripheral tissues and the brain.<sup>[2]</sup> Under normal physiological conditions, S1R complexes with the binding immunoglobulin protein (Bip), a primary ER chaperone protein.<sup>[3]</sup> S1R dissociates from Bip upon ligand activation and translocates to various cellular sites, including mitochondrial and plasma membranes, regulating  $Ca^{++}$  flux and ATP production.<sup>[4]</sup> This regulatory function impacts multiple biological processes and is implicated in the pathophysiology of conditions such as depression, neurodegenerative diseases, and neuropathic pain (NP).<sup>[5]</sup>

S2R, also known as transmembrane protein 97 (TMEM97), is a four-domain transmembrane receptor involved in vital cellular

processes such as cholesterol trafficking, membrane dynamics, autophagy, and receptor stabilization.<sup>[6]</sup> Disruptions in these processes, often triggered by cellular stress, are associated with age-related degenerative diseases, including Alzheimer's disease (AD), Parkinson's disease (PD), and retinal disorders.<sup>[7]</sup> Preclinical and clinical studies suggest that S2R modulators may alleviate neurodegenerative progression and NP conditions.<sup>[8]</sup>

The pharmacophore models for S1R ligands suggest that optimal binding requires a basic amine and an aromatic ring, involving critical interactions with residues such as Glu172 and Tyr206.<sup>[2a,9]</sup> Potent S1R ligands thus feature a positively ionizable center for ionic interactions, and two lipophilic groups for engaging the primary hydrophobic interactions, and an additional hydrophobic interaction within a secondary subpocket.<sup>[10]</sup> Given the role of S1R in central nervous system (CNS) diseases and pain, extensive efforts have focused on developing selective and potent small-molecule S1R ligands (Figure 1). Prominent structural classes include the quinolinomorphans moiety (**1**),<sup>[11]</sup> spirocyclic compounds (**2**, **3**),<sup>[12]</sup> piperazine (**4**, **5**),<sup>[13]</sup> piperidine (**6**),<sup>[10]</sup> azetidines (**7**),<sup>[14]</sup> and pyrrolidine derivatives (**8**),<sup>[15]</sup> all of which have shown high affinity for the S1R. Additionally, non-traditional scaffolds such as in WLB-87848 (**9**) have been explored, which deviate from the standard S1R pharmacophore by featuring a free NH group paired with a lipophilic component.<sup>[16]</sup>

The rich structural diversity of S1R ligands – from straightforward piperazine and piperidine derivatives to complex, multi-ring architectures – provides an exciting opportunity to enhance affinity and selectivity. This work aims to enhance molecular shape control by substituting traditional diamine moieties with rigid bicyclic fused rings, thereby exploring novel bioisosteres (Figure 2). One promising scaffold is tetrahydropyrrolo[3,4-c]pyrazole, a heterocyclic framework with

[a] G. Cosentino, M. Dichiara, G. Costanzo, A. Coco, L. Pasquinucci, A. Marrazzo, A. Rescifina, E. Amata  
University of Catania, Dipartimento di Scienze del Farmaco e della Salute,  
Viale A. Doria 6, 95125 Catania, Italy  
E-mail: maria.dichiara@unisi.it  
eamata@unicat.it

Supporting information for this article is available on the WWW under <https://doi.org/10.1002/cmdc.202401015>

© 2025 The Authors. ChemMedChem published by Wiley-VCH GmbH. This is an open access article under the terms of the Creative Commons Attribution License, which permits use, distribution and reproduction in any medium, provided the original work is properly cited.

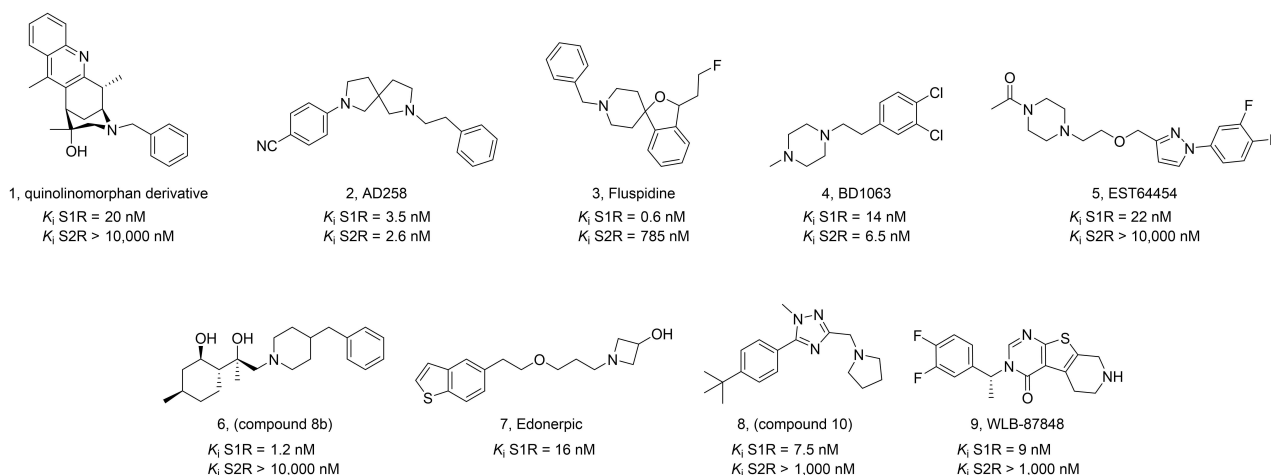


Figure 1. S1R ligands employing different core scaffolds. The number of compounds in round brackets refers to those reported in the original paper.

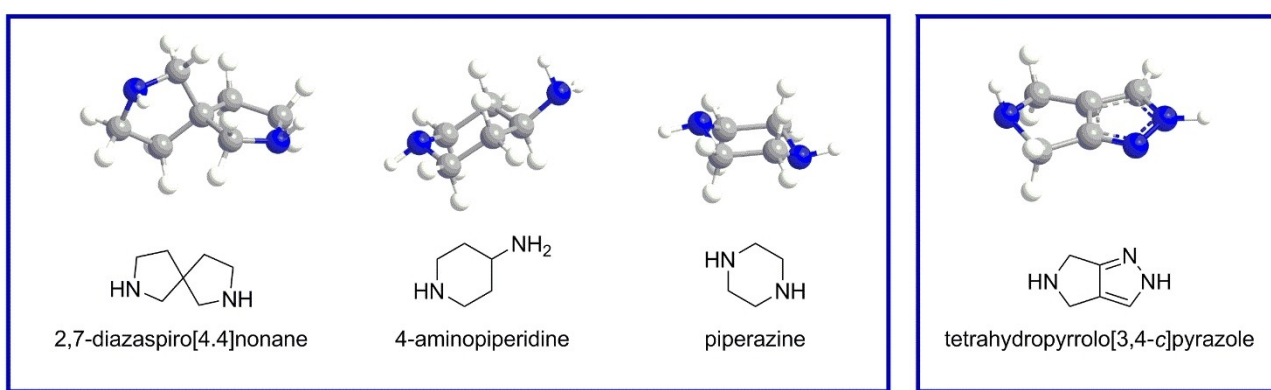


Figure 2. 3D chemical structure of moieties employed as S1R ligands and the tetrahydropyrrolo[3,4-c]pyrazole scaffold.

increased rigidity compared to other moieties and a distinct electronic profile due to its fused pyrazole-pyrrolidine rings.<sup>[21]</sup> The nitrogen atoms within this fused system contribute to a range of binding interactions, including hydrogen bonding, ionic interactions, and  $\pi$ -stacking, all crucial for strong S1R engagement.<sup>[22]</sup> This structural shape may improve the ligand's overall binding properties and allow for a more selective and targeted interaction with the S1R, potentially enhancing pharmacological outcomes.

Moreover, several ligands containing the tetrahydropyrrolo[3,4-c]pyrazole, pyrrolidine, or pyrazole moieties have shown minimal or no inhibition of the  $K^+$  human Ether-à-go-go-Related Gene (hERG) channel,<sup>[23]</sup> a recurring challenge in SR drug development.<sup>[24]</sup> This suggests these derivatives could offer improved selectivity and therapeutic potential without hERG-related cardiotoxicity.

Inspired by these premises, we present our medicinal chemistry efforts in designing S1R ligands based on the tetrahydropyrrolo[3,4-c]pyrazole scaffold. We prepared a set of compounds and built structure-activity relationships (SAR) for SR through radioligand binding assay studies and molecular modeling. These compounds hold promise as pharmacological tools and valuable leads in drug discovery, facilitating deeper

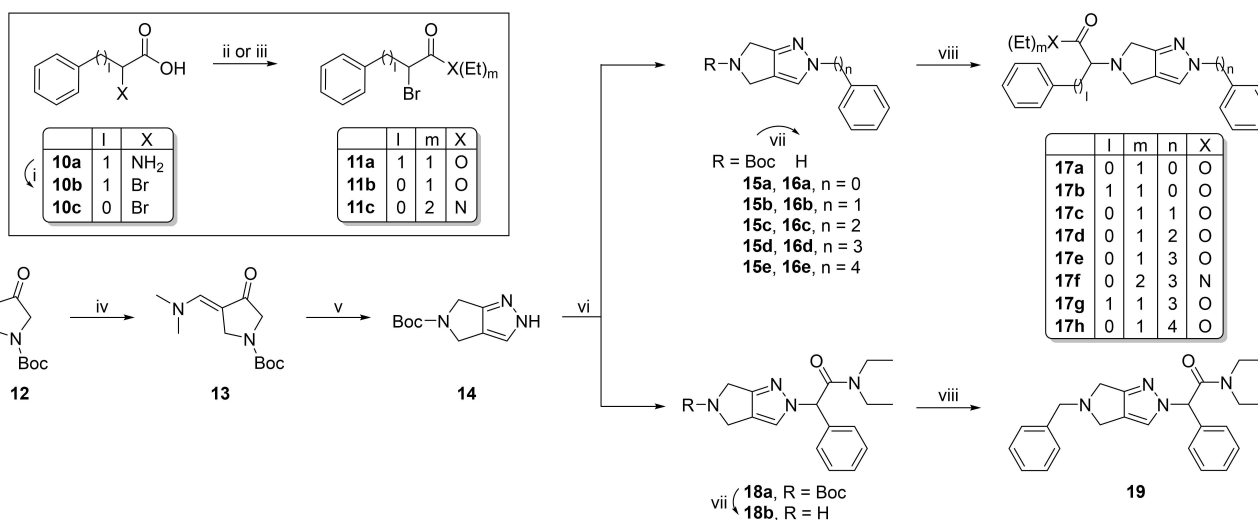
exploration of S1R as a therapeutic target. By potentially minimizing hERG-associated risks, they may offer improved safety profiles for future therapeutic applications.

## 2. Results and Discussion

### 2.1. Chemistry

As reported in Scheme 1, intermediate **11a** was synthesized from commercially available L-phenylalanine (**10a**) by treatment with sodium nitrite under acidic conditions, followed by Fischer esterification.<sup>[25]</sup> Conversely, intermediates **11b,c** were efficiently prepared from  $\alpha$ -bromophenylacetic acid (**10c**). For **11b**, Fischer esterification was conducted in an acid ethanol solution, whereas **11c** was synthesized via acylation using diethylamine.

As regards the 2,4,5,6-tetrahydropyrrolo[3,4-c]pyrazole core (**14**), it was synthesized starting from the commercially available *tert*-butyl 3-oxopyrrolidine-1-carboxylate (**12**) upon treatment with DMF/DMA to provide **13**, and subsequent reaction with hydrazine.<sup>[26]</sup> The alkylation of **14** with opportune bromo-derivatives resulted in **15a–e** and **18a** intermediates. The latter



**Scheme 1.** Reagent and conditions: (i) NaNO<sub>2</sub>, HBr, H<sub>2</sub>O, rt, 2.5 h; (ii) EtOH, H<sub>2</sub>SO<sub>4</sub>, 65 °C, overnight; (iii) 1. SOCl<sub>2</sub>, reflux, 3 h; 2. CH<sub>2</sub>Cl<sub>2</sub>, anhydrous, (Et)<sub>2</sub>NH, DIPEA, rt, overnight; (iv) DMF/DMA, 105 °C; (v) hydrazine monohydrate, BuOH, 127 °C; (vi) K<sub>2</sub>CO<sub>3</sub>, CH<sub>3</sub>CN or DMF, iodobenzene or bromoalkylbenzene or 11c, 50 °C, overnight; (vii) HCl/dioxane 4 M, rt, 8 h; (viii) base, DMF or CH<sub>3</sub>CN, bromo-derivative (11a–c), reflux, overnight.

underwent *N*-Boc removal and further alkylation, resulting in the final derivatives **17a–h** and **19**.

## 2.2. Pharmacological Studies

### 2.2.1. Radioligand Binding Assays

After the synthesis, all the tetrahydropyrrolo[3,4-*c*]pyrazole derivatives were screened for binding affinity to S1R and S2R via radioligand binding assays (Table 1). S1R binding was assessed by displacement of [<sup>3</sup>H](+)-pentazocine and S2R

**Table 1.** SR binding assays for compounds **17a–h**, and **19**.

Compound	K <sub>i</sub> (nM) ± SD <sup>[a]</sup>		
	S1R	S2R	S2R/S1R
<b>17a</b>	344 ± 80	> 10000	> 29
<b>17b</b>	> 10000	> 10000	1
<b>17c</b>	> 10000	> 10000	1
<b>17d</b>	> 10000	> 10000	1
<b>17e</b>	> 10000	> 10000	1
<b>17f</b>	1355 ± 575	> 10000	> 7
<b>17g</b>	> 10000	> 10000	1
<b>17h</b>	> 10000	> 10000	1
<b>19</b>	75 ± 12	431 ± 60	5.7
(+)-PTZ <sup>[b]</sup>	4.3 ± 0.5	1465 ± 224	–
DTG <sup>[b]</sup>	124 ± 19	18 ± 1	–
Haloperidol <sup>[b]</sup>	2.6 ± 0.4	77 ± 18	–
BD1063 <sup>[b]</sup>	14 ± 2.7	204 ± 31	–

[a] Each value is the mean ± SD of at least two experiments performed in duplicate. [b] Taken from reference.<sup>[12]</sup>

binding was measured using [<sup>3</sup>H]DTG. To mitigate the DTG nonselective binding, an excess of non-tritiated (+)-pentazocine was used to block S1R sites.<sup>[12]</sup> Haloperidol and BD1063 were chosen as reference compounds for both S1R and S2R.

The first compound of the series, **17a**, featuring a phenylacetate and phenyl group on either side of the molecule, showed moderate affinity for S1R, with negligible binding for S2R.

Substituent modifications on the pyrazole side were further explored by introducing an alkyl chain between the nitrogen atom and the phenyl ring. This alteration was intended to increase flexibility and adjust the spatial orientation of the ligand within the binding pocket, potentially enhancing interaction with S1R. However, the elongation to phenylmethyl (**17c**), phenylethyl (**17d**), phenylpropyl (**17e**), and phenylbutyl (**17h**) moieties resulted in a complete loss of S1R affinity. Further modifications targeted the nitrogen atom of the tetrahydropyrrole moiety, with the phenylpropanoate derivatives **17b** and **17g** showing no affinity for either SR subtype. In contrast, derivative **17f**, which incorporated an amide functionality, regained S1R affinity in the low micromolar range.

In this latter case, replacing an ester group (as in **17e**) with an amide group (as in **17f**) enhances binding affinity, likely due to the amides' stronger hydrogen-bonding capacity than esters.<sup>[27]</sup>

Next, we expanded the SAR study by swapping the substituents on the two nitrogen atoms. This approach aimed to evaluate how variation in spatial arrangement and steric bulk influence the accessibility and binding efficiency of the tetrahydropyrrole nitrogen within the receptor's binding pocket. This modification led to derivative **19**, demonstrating restored S1R affinity. Notably, **19**, containing a benzyl group, significantly improved S1R affinity, achieving a K<sub>i</sub> value of 75 nM with 6-fold selectivity over S2R.

These findings indicate that substituting the tetrahydropyrrole nitrogen is crucial for modulating binding affinity. Due to its higher basicity than the pyrazole nitrogen, the pyrrolidine nitrogen is likely to be protonated under physiological pH conditions (see paragraph 4.4.1). This protonation facilitates a critical interaction with the carboxylate group of Glu172 within the S1R binding site, forming a stabilizing salt bridge that plays a key role in the ligand's binding affinity and positioning.

In summary, these results underscore the importance of nitrogen accessibility, structural flexibility, and functional group optimization in enhancing S1R affinity. Since compound **19** is a racemic mixture, separating its enantiomers could be a valuable direction for future research. This approach would allow for a more accurate assessment of their individual binding affinities, providing deeper insights into how each enantiomer interacts with the target and potentially enhancing the efficacy or selectivity of the compound. Therefore, this work lays a strong foundation for further refinement of tetrahydropyrrolo[3,4-c]pyrazole derivatives as promising S1R modulators.

### 2.2.2. Preliminary ADMET Profile

To evaluate the therapeutic potential of the synthesized compounds, we employed *in silico* predictions for hERG channel activity, central nervous system (CNS) multiparameter optimization (MPO), and blood-brain barrier (BBB) permeability scores using the advanced features of the MarvinSketch tool. This analysis was conducted for compounds **17a** and **19**, demonstrating superior S1R affinity, and for haloperidol and verapamil, two well-established hERG channel blockers, as reference compounds.<sup>[28]</sup> The results, summarized in Table 2, highlight several key insights.

Compounds **17a** and **19** exhibited low predicted inhibitory activity on the hERG channel, with IC<sub>50</sub> values of 7.24 and 5.37 μM, respectively, categorizing them as safe and with minimal risk of cardiotoxicity. In stark contrast, haloperidol and verapamil displayed an experimental IC<sub>50</sub> of 0.028 μM and 0.14 μM,<sup>[28]</sup> respectively, consistent with the predicted values of 0.06 μM and 0.26 μM, sustaining the accuracy of the predictive model. This significant discrepancy underscores the superior safety profiles of **17a** and **19** compared to haloperidol and verapamil, which are associated with a pronounced risk of cardiotoxicity. Given its S1R affinity profile, an experimental hERG assay was performed on compound **19** to validate these predictions further. The experimental IC<sub>50</sub> of 5.80 μM (Tables 2

and S1) agreed with the predicted value of 5.37 μM, reaffirming the compound's safer profile. Verapamil was used as a reference compound, showing an experimental IC<sub>50</sub> of 0.41 μM.

Compounds **17a** and **19** also achieved CNS MPO scores and BBB permeability scores exceeding 4, indicating their ability to effectively cross the BBB and function at the CNS level (Table 2). These findings collectively highlight a promising safety and efficacy profile for compound **19**. Its low cardiotoxicity risk and ability to penetrate the BBB position it as a candidate for S1R-targeted therapies.

### 2.3. Molecular Modeling Studies

We conducted a comprehensive molecular modeling study to support the experimental findings and the SAR analysis. To this purpose, two distinct X-ray crystallographic structures were selected: the S1R bound to the selective ligand PD144418 (PDB ID: 5HK1) and the S2R in complex with the selective ligand Z4857158944 (PDB ID: 7M96). Since the human S2R structure has not yet been resolved, we constructed a homology model using the bovine S2R structure from the 7M96 template and the Homo sapiens S2R sequence (UniProt entry Q5BJF2).

To validate the molecular modeling approach, docking simulations using AutoDock Vina were performed to reproduce the binding poses and activities of the co-crystallized ligands and haloperidol, a reference compound for both S1R and S2R. This validation confirmed the method's accuracy, as evidenced by the agreement between the docking results and experimental data (Table 3). Following validation, compounds **17a** and **19** were docked in both their protonated and deprotonated forms, considering all possible stereochemical configurations (refer to Section 4.4.1). The docking results (Table 3) correlated well with the experimental data.

A detailed analysis of these docking results revealed distinct interaction preferences for the two compounds. Compound **17a** predominantly interacts in its deprotonated form, while compound **19** favors the protonated state. These observations are consistent with the calculated pK<sub>a</sub> values of the compounds (refer to Section 4.4.1), which increase near a carboxylate ion. This trend aligns with both the experimental data and established findings in the literature.<sup>[29]</sup>

To further understand these binding interactions, we superimposed compounds **17a** and **19** onto their respective co-crystallized ligands, PD144418 and Z4857158944, within the receptor structures. The corresponding active sites are visual-

**Table 2.** ADMET profile of compounds **17a**, **19**, haloperidol, and verapamil.

Compound	hERG exp. (IC <sub>50</sub> , μM, this paper)	hERG exp. (IC <sub>50</sub> , μM)	hERG calcd. (IC <sub>50</sub> , μM)	Classification model	CNS MPO score <sup>[a]</sup>	BBB score <sup>[a]</sup>
<b>17a</b>	–	–	7.24	SAFE	4.75	4.86
<b>19</b>	5.80	–	5.37	SAFE	4.63	4.50
Haloperidol	–	0.028 <sup>b</sup>	0.06	TOXIC	4.81	5.31
Verapamil	0.41	0.14 <sup>b</sup>	0.26	TOXIC	3.09	4.54

[a] A score values ≥ 4.0 on a scale between 0 and 6 suggest CNS drug-likeness and BBB penetration. [b] Taken from reference.<sup>[28]</sup>

**Table 3.** Docking  $K_d$  (nM) SR binding assays for compounds **17a** and **19**.

Compound	S1R		S2R	
	$K_d$ exp.	$K_d$ calcd.	$K_d$ exp.	$K_d$ calcd.
<b>17a</b>	344		> 10000	
( <i>S_C</i> )- <b>17a</b>		111		1065
( <i>R_C</i> )- <b>17a</b>		61.5		1002
( <i>S_C,R_N</i> )- <b>17a</b>		211		764
( <i>S_C,S_N</i> )- <b>17a</b>		176		601
( <i>R_C,R_N</i> )- <b>17a</b>		121		903
( <i>R_C,S_N</i> )- <b>17a</b>		22.2		482
<b>19</b>	75		431	
( <i>S_C</i> )- <b>19</b>		663		1700
( <i>R_C</i> )- <b>19</b>		694		568
( <i>S_C,R_N</i> )- <b>19</b>		279		742
( <i>S_C,S_N</i> )- <b>19</b>		432		657
( <i>R_C,R_N</i> )- <b>19</b>		333		1295
( <i>R_C,S_N</i> )- <b>19</b>		345		1219
PD144418 <sup>[a]</sup>	1.9	47.8	–	–
Z4857158944 <sup>[a]</sup>	–	–	4	16.1
Haloperidol <sup>[b]</sup>	2.6	12.1	77	98.7

[a] Taken from reference.<sup>[30]</sup> [b] Taken from reference.<sup>[12]</sup>

ized in Figure 3. Notably, the S1R binding pocket is fully enclosed (Figure 3, left column), while the S2R pocket remains open, facing the endoplasmic reticulum interior (Figure 3, center and right columns).

Within the S1R binding site, compound **17a**, regardless of protonation state, adopts a specific orientation that positions its linear region toward the cavity containing Glu172 residue. This amino acid is critical for forming a stabilizing salt bridge necessary for optimal ligand-receptor interaction (Figure 3, left column). For the S2R, compound **17a** also fits within the pocket, with its linear portion inside and the bifurcated region extending outward (Figure 3, center column, **17a** in blue). However, due to its orientation, even in its protonated form, **17a** cannot establish the essential salt bridge with Asp29, a key interaction required for S2R-specific ligand activity. In contrast, compound **19**, featuring an inverted phenylacetamide substitution on the pyrazole nitrogen instead of the pyrrolidine nitrogen, adopts a conformation in its protonated form that facilitates salt bridge formation with both Glu172 in S1R and Asp29 in S2R. The protonation of the pyrrolidine nitrogen, enhanced by proximity to the carboxylate ion (refer to Section 4.4.1), contributes to the improved activity of compound **19** on both receptors compared to **17a**.

This analysis is extended to the other compounds within the series, revealing that compounds **17b–g** exhibit negligible affinity for both receptors. This lack of affinity is attributed to their inability to fit optimally within the binding pockets or establish the necessary salt bridges upon protonation. These results highlight the critical role of substituent positioning and scaffold orientation in modulating receptor binding and affinity

and the importance of nitrogen protonation for forming salt bridges with carboxylate residues.

### 3. Conclusions

Our study demonstrates that the tetrahydropyrrolo[3,4-*c*]pyrazole scaffold is a promising structural platform for developing selective S1R ligands. While many structural modifications yielded minimal affinity for both S1R and S2R, these findings highlight the critical influence of specific structural elements on receptor binding. Compound **17a** was a notable advancement, displaying significant S1R affinity ( $K_i = 344$  nM) and inspiring further SAR exploration studies. This led to the discovery of compound **19**, which exhibited a striking increase in S1R affinity ( $K_i = 75$  nM), underscoring the impact of strategic nitrogen substitutions and reduced steric hindrance on receptor engagement. The molecular modeling study provides valuable insights into the compounds' binding interactions. The docking simulations, structural superimpositions, and salt bridge analysis elucidate the factors underlying receptor selectivity and affinity, offering a robust framework to rationalize the experimental findings and guide future ligand design. These findings pave the way for developing safer and more effective S1R modulators as potential therapeutic agents. Given its high affinity and significant binding preference for S1R, compound **19** appears to be a promising candidate for further biological evaluation, particularly due to its reduced inhibition of the hERG  $K^+$  channel.

## Experimental Section

### General Remarks

Reagent-grade chemicals from Merck (Darmstadt, Germany) were used without further purification. Air-sensitive reactions were performed under nitrogen in oven-dried glassware using the syringe-septum cap technique. Purification was done via flash chromatography on Merck silica gel 60 (40–63  $\mu$ m, 230–400 mesh). Electrospray ionization mass spectrometry (ESI-MS) spectra were performed by an Agilent 1100 series LC/MS spectrometer. NMR spectra ( $^1$ H and  $^{13}$ C, 200 and 500 MHz) were recorded on VARIAN INOVA spectrometers in  $CDCl_3$  with TMS as an internal standard. Chemical shifts ( $\delta$ ) are in ppm, and coupling constants (J) are in Hz, with standard multiplicity abbreviations (s = singlet, d = doublet, t = triplet, q = quartet, m = multiplet, br = broad). Microanalysis (C, H, N) using a Carlo Erba E1110 confirmed  $\geq 95\%$  purity for all compounds, within  $\pm 0.4\%$  of theoretical values. TLC was performed on 250  $\mu$ m Merck 60 F<sub>254</sub> silica gel plates, with spots visualized under UV, permanganate, or iodine. The nomenclature of the chemical compounds was generated with ChemBioDraw Ultra 16.0.0.82.

### Synthetic Procedures

#### General Procedure for Amine Preparation (Procedure A)

To a solution of **14** (1.00 eq) in anhydrous DMF or  $CH_3CN$  (120 mM),  $K_2CO_3$  (2.50 eq) and bromo-derivative (1.50 eq) were sequentially

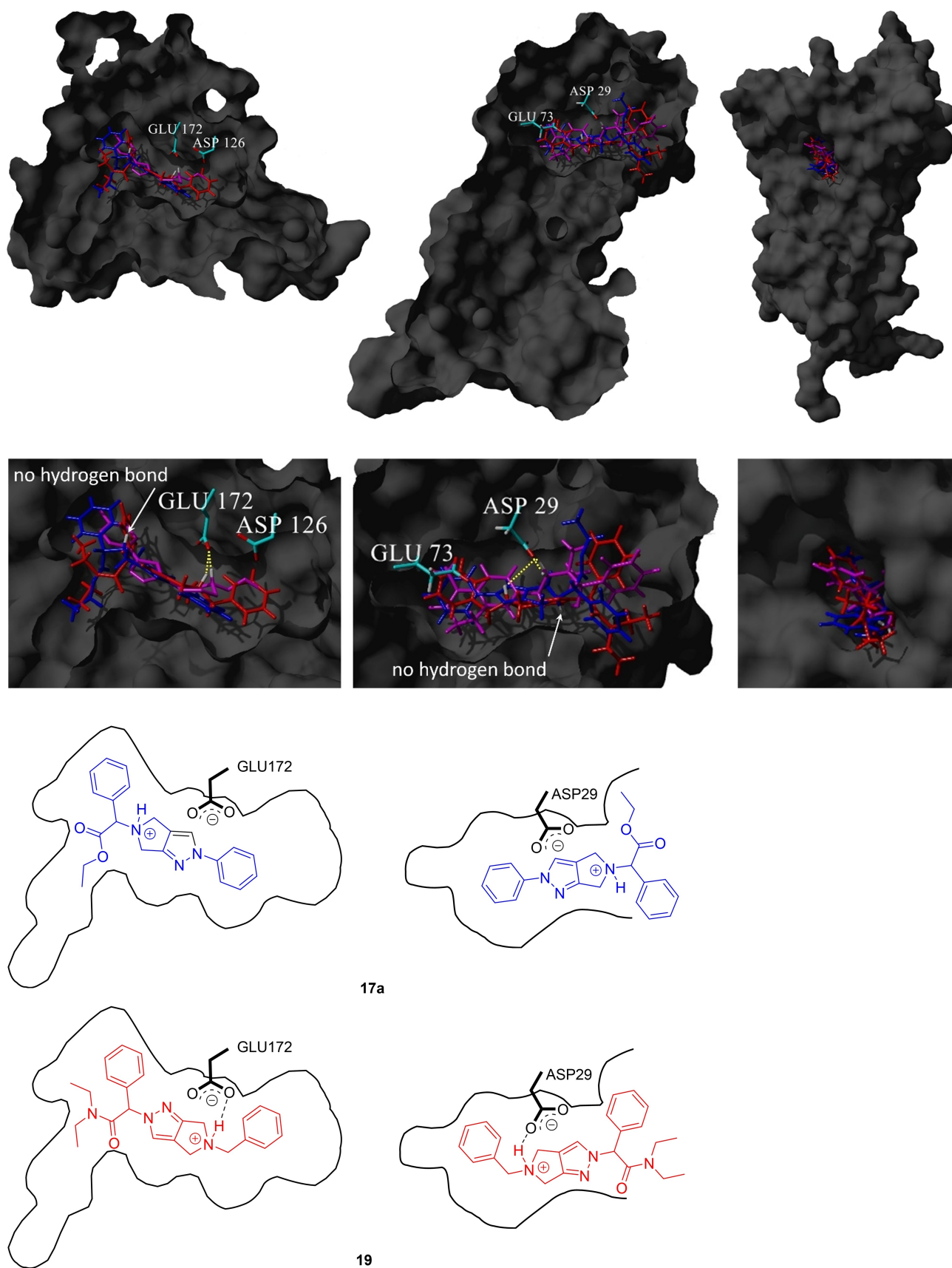


**Figure 3.** Cross-section of the S1R (upper left) and S2R (upper center) receptor-binding pocket with the respective co-crystallized ligands PD144418 and Z4857158944 (magenta) and docked 17a and 19 compounds (blue and red, respectively). View of the entrance for S2R to the binding pocket from the membrane (upper right). Enlarged view of upper scenes (center). 2D graphical sketches of compounds 17a and 19 within the S1R (bottom left) and S2R (bottom center) binding pockets.

added. The reaction has been left to stir at 50 °C overnight. After completion, the reaction mixture was concentrated *in vacuo*, the residue dissolved in EtOAc (20 mL), washed with a saturated solution of NaHCO<sub>3</sub> (1×10 mL), brine (1×5 mL), dried over anhydrous Na<sub>2</sub>SO<sub>4</sub>, filtered and evaporated to dryness. The residue was purified via silica gel chromatography to obtain the desired product. Products synthesized according to this procedure are **15a–e** and **18a**.

### General Procedure for Amine Preparation (Procedure B)

The solution of *N*-Boc-protected amine (1.00 eq) in CH<sub>2</sub>Cl<sub>2</sub> has been stirred with 4 M HCl in dioxane (10.0 eq) at rt for 8 h. After completion, the solvent was removed under pressure, and the residue was washed with CH<sub>2</sub>Cl<sub>2</sub> (2×1 mL), concentrated *in vacuo*, and used for the next step. Products synthesized according to this procedure are **16a–e** and **18b**. The resulting amine was dissolved in DMF or CH<sub>3</sub>CN (100 mM). Subsequently, K<sub>2</sub>CO<sub>3</sub>, Cs<sub>2</sub>CO<sub>3</sub>, or DIPEA (2.50 eq) and appropriate bromo-derivative (1.50 eq) were added. The reaction mixture was stirred under reflux overnight. After completion, the reaction mixture was concentrated *in vacuo*, the residue dissolved in EtOAc (20 mL), washed with a saturated solution of NaHCO<sub>3</sub> (1×10 mL), brine (1×5 mL), dried over anhydrous Na<sub>2</sub>SO<sub>4</sub>, filtered and evaporated to dryness. The residue was purified via silica gel chromatography to obtain the desired product. The products synthesized according to this procedure are **17a–e**, **19**.

### General Procedure for Oxalate Salts Formation (Procedure C)

For all final compounds, the pure product (1.00 eq) was dissolved in EtOAc, and a solution of oxalic acid (1.00 eq) in EtOAc was added dropwise at 0 °C to obtain the desired product as oxalate salt.

### Synthesis and Characterization of All Compounds

**2-Bromo-3-phenylpropanoic acid (10b)**. L-Phenylalanine (**10a**) (507 mg, 3.07 mmol, 1.00 eq) was dissolved in H<sub>2</sub>O (1.38 mL, 2.20 M) and cooled to 0 °C. Then, 47% HBr (w/w) (1.50 mL, 27.6 mmol, 9.00 eq) was added, followed by NaNO<sub>2</sub> (339 mg, 4.91 mmol, 1.60 eq) water solution (0.75 mL, 6.50 M). The mixture was stirred at 0 °C for 0.5 h and at rt for 2.5 h. After completion, the reaction mixture was concentrated *in vacuo*, the residue dissolved in Et<sub>2</sub>O (20 mL), washed with brine (1×7 mL), dried over anhydrous Na<sub>2</sub>SO<sub>4</sub>, filtered, and concentrated *in vacuo* to obtain a colorless oil which was used as it without further purification.

**Ethyl 2-bromo-3-phenylpropanoate (11a)**. To a solution of **10b** (424 mg, 1.85 mmol, 1.00 eq) in EtOH (15 mL, 123 mM), H<sub>2</sub>SO<sub>4</sub> (95–97% w/w, 126 μL, 2.31 mmol, 1.25 eq) was added dropwise and the reaction mixture left to stir overnight at 65 °C. After completion, the reaction mixture was concentrated *in vacuo*, the residue dissolved in EtOAc (30 mL), washed with a saturated solution of NaHCO<sub>3</sub> (1×10 mL), brine (1×10 mL), dried over anhydrous Na<sub>2</sub>SO<sub>4</sub>, filtered and concentrated *in vacuo*. The residue was purified by flash chromatography using hexane/CH<sub>2</sub>Cl<sub>2</sub> as eluent (90:10 to 85:15). Light yellow oil, yield 270 mg (57%), C<sub>11</sub>H<sub>13</sub>BrO<sub>2</sub> (257.1 g mol<sup>-1</sup>). <sup>1</sup>H NMR (500 MHz, CDCl<sub>3</sub>) δ 7.16–7.37 (m, 5H), 4.39 (t, *J* = 7.8 Hz, 1H), 4.17 (q, *J* = 7.2 Hz, 2H), 3.46 (q, *J* = 7.0 Hz, 1H), 3.24 (q, *J* = 7.0 Hz, 1H), 1.22 (t, *J* = 7.2 Hz, 3H).<sup>[32]</sup>

**Ethyl 2-bromo-2-phenylacetate (11b)**. To a solution of α-bromo-phenylacetic acid (**10c**) (500 mg, 2.33 mmol, 1.00 eq) in EtOH (9 mL, 240 mM), H<sub>2</sub>SO<sub>4</sub> (95–97% p/v, 158 μL, 2.91 mmol, 1.25 eq) was added at rt. The reaction mixture was stirred at 100 °C for 5 h. After completion, the reaction mixture was concentrated *in vacuo*, the

residue dissolved in EtOAc (15 mL), washed with a saturated solution of NaHCO<sub>3</sub> (1×5 mL), brine (1×5 mL), dried over anhydrous Na<sub>2</sub>SO<sub>4</sub>, filtered and concentrated *in vacuo*. The residue was purified by flash chromatography using PE/EtOAc (100:0 to 99:1). Clear oil, yield 485 mg (85%), C<sub>10</sub>H<sub>11</sub>BrO<sub>2</sub> (243.1 g mol<sup>-1</sup>). <sup>1</sup>H NMR (500 MHz, CDCl<sub>3</sub>) δ 7.54–7.58 (m, 2H), 7.33–7.41 (m, 3H), 5.35 (s, 1H), 4.19–4.32 (m, 2H), 1.30 (t, *J* = 7.1 Hz, 3H).<sup>[33]</sup>

**2-Bromo-*N,N*-diethyl-2-phenylacetamide (11c)**. A solution of α-bromo-phenylacetic acid (**10c**) (500 mg, 2.33 mmol, 1.00 eq) in thionyl chloride (1.69 mL, 23.3 mmol, 10.0 eq) was refluxed for 5.5 h. After completion, the excess of thionyl chloride was distilled, and the reaction mixture was washed with CH<sub>2</sub>Cl<sub>2</sub> anhydrous (3×1 mL). The resulting acyl chloride was then dissolved in anhydrous CH<sub>2</sub>Cl<sub>2</sub> (3 mL, 766 mM), diethylamine (289 μL, 2.79 mmol, 1.20 eq) and DIPEA (486 μL, 2.79 mmol, 1.20 eq) were added at 0 °C, and the reaction mixture was stirred at rt overnight. After completion, the reaction mixture was concentrated *in vacuo*, the residue dissolved in EtOAc (15 mL), washed with a saturated solution of NaHCO<sub>3</sub> (1×5 mL), brine (1×5 mL), dried over anhydrous Na<sub>2</sub>SO<sub>4</sub>, filtered and concentrated *in vacuo*. The residue was purified by flash column chromatography using PE/EtOAc (90:10 to 85:15). Pale yellow oil, yield 220 mg (35%), C<sub>12</sub>H<sub>16</sub>BrNO (270.2 g mol<sup>-1</sup>). <sup>1</sup>H NMR (500 MHz, CDCl<sub>3</sub>) δ 7.43–7.56 (m, 2H), 7.30–7.43 (m, 3H), 5.65 (s, 1H), 3.27–3.46 (m, 4H), 1.13 (td, *J* = 7.3, 18.7 Hz, 6H).<sup>[34]</sup>

***tert*-Butyl (E)-3-[(dimethylamino)methylene]-4-oxopyrrolidine-1-carboxylate (12)**. A solution of *tert*-butyl 3-oxopyrrolidine-1-carboxylate (**12**) (5.00 g, 26.99 mmol, 1.00 eq) in DMF-DMA (35.94 mL, 270 mmol, 10.00 eq) was stirred at 105 °C for 3 h. After completion, the reaction mixture was concentrated *in vacuo*, the residue triturated with hexane (20 mL) and filtered under vacuum. Brown solid, yield 5.6 g (86%), C<sub>12</sub>H<sub>20</sub>N<sub>2</sub>O<sub>3</sub> (240.3 g mol<sup>-1</sup>). <sup>1</sup>H NMR (200 MHz, CDCl<sub>3</sub>) δ 7.31 (s, 1H), 4.55 (d, *J* = 9.0 Hz, 2H), 3.83 (d, *J* = 9.3 Hz, 2H), 3.10 (s, 6H), 1.48 (s, 9H).<sup>[35]</sup>

***tert*-Butyl 2,6-dihydropyrrolo[3,4-*c*]pyrazole-5(4*H*)-carboxylate (14)**. To a solution of **13** (5.60 g, 23.30 mmol, 1.00 eq) in butanol (26 mL, 900 mM), hydrazine hydrochloride (16.00 g, 233 mmol, 10.00 eq) was added. The reaction mixture was stirred under reflux for 6 h. After completion, the mixture was concentrated *in vacuo*, the residue dissolved in CH<sub>2</sub>Cl<sub>2</sub> (20 mL), washed with a saturated solution of NaHCO<sub>3</sub> (1×15 mL), brine (1×15 mL), dried over anhydrous Na<sub>2</sub>SO<sub>4</sub>, filtered and concentrated *in vacuo*. The residue was purified by flash column chromatography using CHCl<sub>3</sub>/EtOAc (60:40 to 50:50). White solid, yield 2.3 g (48%), C<sub>10</sub>H<sub>15</sub>N<sub>3</sub>O<sub>2</sub> (209.3 g mol<sup>-1</sup>). <sup>1</sup>H NMR (200 MHz, CDCl<sub>3</sub>) δ 7.32 (d, *J* = 6.3 Hz, 1H), 4.40–4.56 (m, 4H), 1.53 (s, 9H).<sup>[23f,26b]</sup>

***tert*-Butyl 2-phenyl-2,6-dihydropyrrolo[3,4-*c*]pyrazole-5(4*H*)-carboxylate (15a)**. To a solution of **14** (125 mg, 0.60 mmol, 1.00 eq) in anhydrous dioxane (120 mM), iodobenzene (171 mg, 0.84 mmol, 1.40 eq) was added. Then, Cs<sub>2</sub>CO<sub>3</sub> (487 mg, 1.39 mmol, 2.50 eq), KI (10 mg, 0.06 mmol, 0.10 eq), and CuI (12 mg, 0.06 mmol, 0.10 eq) have been sequentially added. The reaction has been left to stir at 120 °C for 48 h. After completion, the mixture was concentrated *in vacuo*, the residue dissolved in EtOAc (20 mL), washed with 15% NH<sub>4</sub>OH solution (1×10 mL), brine (1×10 mL), dried over anhydrous Na<sub>2</sub>SO<sub>4</sub>, filtered and evaporated to dryness. The residue was purified by flash chromatography using hexane/acetone (90:10). Light yellow oil, yield 60 mg (35%), C<sub>16</sub>H<sub>19</sub>N<sub>3</sub>O<sub>2</sub> (285.4 g mol<sup>-1</sup>). <sup>1</sup>H NMR (200 MHz, CDCl<sub>3</sub>) δ 7.55–7.74 (m, 3H), 7.37–7.51 (m, 2H), 7.20–7.34 (m, 1H), 4.45–4.62 (m, 4H), 1.53 (s, 9H).<sup>[36]</sup>

***tert*-Butyl 2-benzyl-2,6-dihydropyrrolo[3,4-*c*]pyrazole-5(4*H*)-carboxylate (15b)**. The compound has been prepared using **14** (132 mg, 0.63 mmol, 1.00 eq) and (bromomethyl)benzene (173 mg, 1.01 mmol, 1.60 eq) following procedure A. The residue was

purified by flash chromatography using hexane/EtOAc (100:0 to 80:20). Pale yellow oil, yield 68 mg (36%).  $C_{17}H_{21}N_3O_2$  (299.4 g mol<sup>-1</sup>). <sup>1</sup>H NMR (200 MHz, CDCl<sub>3</sub>) δ 7.16–7.42 (m, 6H), 5.23 (s, 2H), 4.28–4.42 (m, 2H), 4.07–4.18 (m, 2H), 1.47 (s, 9H).

*tert*-Butyl 2-(*phenethyl*-2,6-dihydropyrrolo[3,4-*c*]pyrazole-5(4*H*)-carboxylate (15*c*). The compound has been prepared using **14** (131 mg, 0.62 mmol, 1.00 eq) and (2-bromoethyl)benzene (174 mg, 0.94 mmol, 1.50 eq) following procedure A. The residue was purified by flash chromatography using hexane/EtOAc (100:0 to 80:20). Colorless oil, yield 103 mg (52%).  $C_{18}H_{23}N_3O_2$  (313.4 g mol<sup>-1</sup>). <sup>1</sup>H NMR (200 MHz, CDCl<sub>3</sub>) δ 7.20–7.36 (m, 3H), 7.09 (d, *J* = 7.4 Hz, 2H), 6.89 (s, 1H), 4.25–4.54 (m, 6H), 3.15 (t, *J* = 7.2 Hz, 2H), 1.51 (d, *J* = 1.6 Hz, 9H).

*tert*-Butyl 2-(3-phenylpropyl)-2,6-dihydropyrrolo[3,4-*c*]pyrazole-5(4*H*)-carboxylate (15*d*). The compound has been prepared using **14** (500 mg, 2.39 mmol, 1.00 eq) and (3-bromopropyl)benzene (556 mg, 2.81 mmol, 1.20 eq) following procedure A. The residue was purified by flash chromatography using hexane/EtOAc (80:20). Colorless oil, yield 288 mg (37%).  $C_{19}H_{25}N_3O_2$  (327.4 g mol<sup>-1</sup>). <sup>1</sup>H NMR (200 MHz, CDCl<sub>3</sub>) δ 7.12–7.34 (m, 5H), 7.08 (s, 1H), 4.38–4.52 (m, 4H), 4.09 (t, *J* = 7.0 Hz, 2H), 2.61 (t, *J* = 8.0 Hz, 2H), 2.19 (quin, *J* = 7.2 Hz, 2H), 1.51 (s, 9H).

*tert*-Butyl 2-(4-phenylbutyl)-2,6-dihydropyrrolo[3,4-*c*]pyrazole-5(4*H*)-carboxylate (15*e*). The compound has been prepared using **14** (150 mg, 0.72 mmol, 1.00 eq) and (4-bromobutyl)benzene (198 mg, 0.93 mmol, 1.30 eq) following procedure A. The residue was purified by flash chromatography using hexane/EtOAc (85:15). Colorless oil, yield 80 mg (33%).  $C_{20}H_{27}N_3O_2$  (341.5 g mol<sup>-1</sup>). <sup>1</sup>H NMR (200 MHz, CDCl<sub>3</sub>) δ 7.11–7.35 (m, 5H), 7.07 (s, 1H), 4.37–4.50 (m, 4H), 4.10 (t, *J* = 6.7 Hz, 2H), 2.63 (t, *J* = 7.5 Hz, 2H), 1.80–1.98 (m, 2H), 1.61 (t, *J* = 7.30 Hz, 2H), 1.50 (s, 9H).

*Ethyl* 2-phenyl-2-(2-phenyl-2,6-dihydropyrrolo[3,4-*c*]pyrazol-5(4*H*)-yl)acetate (17*a*). The compound has been prepared using **16a** (130 mg, 0.45 mmol, 1.00 eq) and **11b** (164 mg, 0.68 mmol, 1.50 eq) following procedure B. The residue was purified by flash chromatography using hexane/EtOAc (85:15). Colorless oil, yield 157 mg (63%). Anal. calcd for  $C_{21}H_{21}N_3O_2$ : C, 72.60; H, 6.09; N, 12.10; Found: C, 73.01; H, 6.11; N, 12.15. ESI-MS *m/z* 348.1 [M+H]<sup>+</sup>. <sup>1</sup>H NMR (500 MHz, CDCl<sub>3</sub> – free base) δ 7.60 (d, *J* = 7.8 Hz, 2H), 7.46–7.56 (m, 3H), 7.31–7.44 (m, 5H), 7.18–7.27 (m, 1H), 4.57 (s, 1H), 4.15–4.26 (m, 2H), 3.94–3.99 (m, 1H), 3.82–3.93 (m, 3H), 1.18–1.32 (m, 3H). <sup>13</sup>C NMR (126 MHz, DMSO-*d*<sub>6</sub>) δ 171.4, 158.9, 140.7, 136.7, 129.4, 128.8, 128.7, 128.6, 128.5, 126.0, 123.0, 119.7, 119.1, 118.8, 72.3, 61.1, 49.9, 49.4, 14.1.

*Ethyl* 3-phenyl-2-(2-phenyl-2,6-dihydropyrrolo[3,4-*c*]pyrazol-5(4*H*)-yl)propanoate (17*b*). The compound has been prepared using **16a** (60 mg, 0.21 mmol, 1.00 eq) and **11a** (74 mg, 0.29 mmol, 1.35 eq) following procedure B. The residue was purified by flash chromatography using hexane/EtOAc (85:15). Colorless oil, yield 10 mg (13%). Anal. calcd for  $C_{22}H_{23}N_3O_2$ : C, 73.11; H, 6.41; N, 11.63; Found: C, 73.75, H, 6.44; N, 11.70. ESI-MS *m/z* 362.1 [M+H]<sup>+</sup>, 384.2 [M+Na]<sup>+</sup>. <sup>1</sup>H NMR (500 MHz, CDCl<sub>3</sub> – free base) δ 7.51–7.66 (m, 3H), 7.37–7.47 (m, 2H), 7.17–7.34 (m, 6H), 4.20 (d, *J* = 11.7 Hz, 1H), 4.01–4.16 (m, 5H), 3.86 (t, *J* = 7.6 Hz, 1H), 3.08–3.23 (m, 2H), 1.15 (t, *J* = 7.1 Hz, 3H). <sup>13</sup>C NMR (126 MHz, CDCl<sub>3</sub> – free base) δ 172.3, 158.9, 140.7, 137.9, 129.4 (2 C), 129.0 (2 C), 128.4 (2 C), 126.5, 125.9, 123.0, 119.6 (2 C), 118.9, 66.3, 60.4, 48.1, 47.8, 37.2, 14.3.

*Ethyl* 2-(2-benzyl-2,6-dihydropyrrolo[3,4-*c*]pyrazol-5(4*H*)-yl)-2-phenylacetate (17*c*). The compound has been prepared using **16b** (74 mg, 0.25 mmol, 1.00 eq) and **11b** (86 mg, 0.35 mmol, 1.30 eq) following procedure B. The residue was purified by flash column chromatography using hexane/EtOAc (80:20). Yellow oil, yield 10 mg (5%). Anal. calcd for  $C_{22}H_{23}N_3O_2$ : C, 73.11, H, 6.41, N, 11.63; Found: C,

73.53; H, 6.43, N, 11.69. ESI-MS *m/z* 362.2 [M+H]<sup>+</sup>, 384.1 [M+Na]<sup>+</sup>, 400.2 [M+K]<sup>+</sup>. <sup>1</sup>H NMR (500 MHz, CDCl<sub>3</sub> – free base) δ 7.44 (dd, *J* = 1.7, 7.6 Hz, 2H), 7.25–7.38 (m, 6H), 7.19 (s, 1H), 7.14–7.18 (m, 2H), 5.15 (d, *J* = 2.5 Hz, 2H), 4.48 (s, 1H), 4.09–4.23 (m, 2H), 3.77 (tq, *J* = 2.1, 10.5 Hz, 2H), 3.62–3.67 (m, 1H), 3.55–3.61 (m, 1H), 1.19 (t, *J* = 7.1 Hz, 3H). <sup>13</sup>C NMR (126 MHz, CDCl<sub>3</sub> – free base) δ 171.3, 145.3, 136.7, 135.9, 131.8, 128.8 (2 C), 128.7 (2 C), 128.5 (2 C), 128.4 (2 C), 128.0, 127.8, 123.1, 72.1, 61.0, 54.8, 50.3, 49.1, 14.1.

*Ethyl* 2-(2-phenethyl-2,6-dihydropyrrolo[3,4-*c*]pyrazol-5(4*H*)-yl)-2-phenylacetate (17*d*). The compound has been prepared using **16c** (70 mg, 0.22 mmol, 1.00 eq) and **11b** (72 mg, 0.30 mmol, 1.30 eq) following procedure B. The residue was purified by flash chromatography using hexane/EtOAc (90:10 to 75:25). Pale yellow oil, yield 29 mg (34%). Anal. calcd for  $C_{23}H_{25}N_3O_2$ : C, 73.57, H, 6.71, N, 11.19; Found: C, 74.22, H, 6.75, N, 11.27. ESI-MS *m/z* 376.2 [M+H]<sup>+</sup>. <sup>1</sup>H NMR (200 MHz, CDCl<sub>3</sub> – free base) δ 7.46–7.59 (m, 2H), 7.18–7.42 (m, 6H), 7.05–7.15 (m, 2H), 6.80 (s, 1H), 4.52 (s, 1H), 4.10–4.32 (m, 4H), 3.85 (q, *J* = 11.7 Hz, 2H), 3.73 (s, 2H), 3.10 (t, *J* = 7.2 Hz, 2H), 1.17–1.28 (m, 3H). <sup>13</sup>C NMR (50 MHz, CDCl<sub>3</sub> – free base) δ 171.5, 156.7, 138.2, 136.8, 128.7 (2 C), 128.6 (2 C), 128.5 (2 C), 128.4 (2 C), 126.5 (2 C), 122.2, 120.2, 72.5, 61.0, 53.7, 50.2, 49.7, 37.3, 14.1.

*Ethyl* 2-phenyl-2-[2-(3-phenylpropyl)-2,6-dihydropyrrolo[3,4-*c*]pyrazol-5(4*H*)-yl]acetate (17*e*). The compound has been prepared using **16d** (77 mg, 0.24 mmol, 1.00 eq) and **11b** (86 mg, 0.35 mmol, 1.50 eq) following procedure B. The residue was purified by flash chromatography using hexane/EtOAc (80:20 to 75:25). Colorless oil, yield 11 mg (12%). Anal. calcd for  $C_{24}H_{27}N_3O_2$ : C, 74.01, H, 6.99, N, 10.79; Found: C, 74.55, H, 7.03, N, 10.81. ESI-MS *m/z* 390.2 [M+H]<sup>+</sup>. <sup>1</sup>H NMR (500 MHz, CDCl<sub>3</sub> – free base) δ 7.50 (dd, *J* = 1.2, 8.1 Hz, 2H), 7.32–7.42 (m, 3H), 7.23–7.29 (m, 2H), 7.10–7.20 (m, 4H), 4.54 (s, 1H), 4.13–4.26 (m, 2H), 3.95 (t, *J* = 7.1 Hz, 2H), 3.74–3.88 (m, 4H), 2.59 (t, *J* = 8.0 Hz, 2H), 2.11 (quin, *J* = 7.3 Hz, 2H), 1.22 (t, *J* = 7.1 Hz, 3H). <sup>13</sup>C NMR (126 MHz, CDCl<sub>3</sub> – free base) δ 171.8, 156.8, 141.2, 137.2, 128.9 (2 C), 128.9 (2 C), 128.7 (2 C), 126.3 (2 C), 126.3 (2 C), 122.4, 120.6, 72.8, 61.3, 51.7, 50.5, 50.1, 32.9, 32.3, 14.4.

*N,N*-Diethyl-2-phenyl-2-[2-(3-phenylpropyl)-2,6-dihydropyrrolo[3,4-*c*]pyrazol-5(4*H*)-yl]acetamide (17*f*). The compound has been prepared using **16d** (155 mg, 0.47 mmol, 1.00 eq) and **11c** (184 mg, 0.68 mmol, 1.50 eq) following procedure B. The residue was purified by flash chromatography using hexane/EtOAc (40:60). Colorless oil, yield 11 mg (12%).  $C_{26}H_{32}N_4O$  (416.6 g mol<sup>-1</sup>). ESI-MS *m/z* 417.2 [M+H]<sup>+</sup>. <sup>1</sup>H NMR (200 MHz, CDCl<sub>3</sub> – free base) δ 7.09–7.55 (m, 10H), 6.96 (s, 1H), 4.79 (s, 1H), 4.04 (t, *J* = 7.0 Hz, 2H), 3.72–3.99 (m, 4H), 3.02–3.63 (m, 4H), 2.57 (t, *J* = 8.2 Hz, 2H), 2.16 (quin, *J* = 7.8 Hz, 2H), 1.12 (t, *J* = 7.0 Hz, 3H), 1.01 (t, *J* = 7.2 Hz, 3H). <sup>13</sup>C NMR (50 MHz, CDCl<sub>3</sub> – free base) δ 141.2, 129.2 (2 C), 129.1 (2 C), 128.9 (2 C), 128.8 (2 C), 128.6 (2 C), 128.6, 128.3, 128.2, 126.1, 122.2, 51.6, 50.0, 49.3, 41.5, 40.5, 32.8, 32.3, 14.3, 13.0.

*Ethyl* 3-phenyl-2-[2-(3-phenylpropyl)-2,6-dihydropyrrolo[3,4-*c*]pyrazol-5(4*H*)-yl]propanoate (17*g*). The compound has been prepared using **16d** (155 mg, 0.47 mmol, 1.00 eq) and **11a** (121 mg, 0.47 mmol, 1.00 eq) following procedure B. The residue was purified by flash column chromatography using hexane/acetone (90:10). Colorless oil, yield 11 mg (6%). Anal. calcd for  $C_{25}H_{29}N_3O_2$ : C, 74.41, H, 7.24, N, 10.41; Found: C, 74.98, H, 7.30, N, 10.47. ESI-MS *m/z* 404.2 [M+H]<sup>+</sup>, 426.2 [M+Na]<sup>+</sup>. <sup>1</sup>H NMR (200 MHz, CDCl<sub>3</sub> – free base) δ 7.18–7.36 (m, 9H), 7.15 (s, 1H), 7.02 (s, 1H), 4.09–4.18 (m, 2H), 4.05 (dd, *J* = 2.2, 7.2 Hz, 4H), 3.90–4.01 (m, 2H), 3.83 (t, *J* = 7.6 Hz, 1H), 3.02–3.25 (m, 2H), 2.61 (t, *J* = 7.8 Hz, 2H), 2.18 (quin, *J* = 7.2 Hz, 2H), 1.12 (t, *J* = 7.2 Hz, 3H). <sup>13</sup>C NMR (126 MHz, CDCl<sub>3</sub> – free base) δ 172.3, 156.5, 140.9, 137.9, 129.0 (2 C), 128.4 (2 C), 128.3 (2 C), 126.5 (2 C), 126.0 (2 C), 122.1, 120.3, 66.5, 60.3, 51.5, 48.3, 48.1, 37.3, 32.6, 32.0, 14.2.

*Ethyl 2-phenyl-2-[2-(4-phenylbutyl)-2,6-dihydropyrrolo[3,4-c]pyrazol-5(4H)-yl]acetate (17h)*. The compound has been prepared using **16e** (80 mg, 0.23 mmol, 1.00 eq) and **11b** (72 mg, 0.29 mmol, 1.30 eq) following procedure B. The residue was purified by flash chromatography using hexane/EtOAc (80:20 to 75:25). Yellow oil, yield 34 mg (37%). Anal. calcd for  $C_{25}H_{29}N_3O_2$ : C, 74.41, H, 7.24, N, 10.41; Found: C, 74.95, H, 7.29, N, 10.49. ESI-MS  $m/z$  404.2  $[M+H]^+$ .  $^1H$  NMR (200 MHz,  $CDCl_3$  – free base)  $\delta$  7.47–7.59 (m, 2H), 7.05–7.46 (m, 8H), 6.96 (s, 1H), 4.51 (s, 1H), 4.11–4.28 (m, 2H), 4.05 (t,  $J=6.8$  Hz, 2H), 3.67–3.93 (m, 4H), 2.61 (t,  $J=7.5$  Hz, 2H), 1.72–1.97 (m, 2H), 1.51–1.71 (m, 2H), 1.23 (t,  $J=7.1$  Hz, 3H).  $^{13}C$  NMR (50 MHz,  $CDCl_3$  – free base)  $\delta$  171.6, 156.5, 142.0, 137.0, 128.8 (2 C), 128.7 (2 C), 128.5 (2 C), 128.4 (2 C), 126.0 (2 C), 122.2, 120.5, 72.7, 61.2, 52.3, 50.3, 49.9, 35.5, 30.5, 28.5, 14.3.

*tert-Butyl-2-[2-(diethylamino)-2-oxo-1-phenylethyl]-2,6-dihydropyrrolo[3,4-c]pyrazole-5(4H)-carboxylate (18a)*. Compound **14** (400 mg, 1.91 mmol, 1.00 eq) was dissolved in a mixture of anhydrous  $CH_3CN/DMF$  (4.80 mL, 4:1 v/v). Then, **11c** (517 mg, 2.29 mmol, 1.20 eq) and  $K_2CO_3$  (528 mg, 3.82 mmol, 2.00 eq) were added, and the mixture was left to stir overnight at rt. After completion, the reaction mixture was concentrated *in vacuo*, the residue dissolved in EtOAc (15 mL), washed with a saturated solution of  $NaHCO_3$  (1 $\times$ 5 mL), brine (1 $\times$ 5 mL), dried over anhydrous  $Na_2SO_4$ , filtered and concentrated *in vacuo*. The residue was purified by flash chromatography using PE/EtOAc (60:40). Light yellow oil, yield 277 mg (36%).  $C_{22}H_{30}N_4O_3$  (398.5  $g\ mol^{-1}$ ).  $^1H$  NMR (200 MHz,  $CDCl_3$ )  $\delta$  7.36–7.49 (m, 5H), 7.12 (s, 1H), 6.43 (s, 1H), 4.20–4.59 (m, 4H), 3.61 (dd,  $J=6.8, 13.5$  Hz, 1H), 3.08–3.41 (m, 3H), 1.47 (s, 9H), 1.12–1.19 (m, 3H), 1.04–1.11 (m, 3H).

*2-[5-Benzyl-5,6-dihydropyrrolo[3,4-c]pyrazol-2(4H)-yl]-N,N-diethyl-2-phenylacetamide (19)*. The compound has been prepared using **18a** (85 mg, 0.21 mmol, 1.00 eq) and (chloromethyl)benzene (36 mg, 0.29 mmol, 1.30 eq) following procedure B. The residue was purified by flash chromatography using EtOAc. Pale yellow oil, yield 9.5 mg (11%). Anal. calcd for  $C_{24}H_{28}N_4O$ : C, 74.20, H, 7.26, N, 14.42; Found: 74.73, H, 7.31, N, 14.52. ESI-MS  $m/z$  389.2  $[M+H]^+$ .  $^1H$  NMR (200 MHz,  $CDCl_3$  – free base)  $\delta$  7.34–7.43 (m, 7H), 7.27–7.34 (m, 2H), 7.23 (d,  $J=7.8$  Hz, 1H), 7.07 (s, 1H), 6.41 (s, 1H), 3.93 (s, 2H), 3.82 (d,  $J=8.2$  Hz, 2H), 3.66–3.75 (m, 2H), 3.53–3.65 (m, 1H), 3.18–3.37 (m, 3H), 1.15–1.21 (m, 3H), 1.08–1.15 (m, 3H).  $^{13}C$  NMR (50 MHz,  $CDCl_3$  – free base)  $\delta$  167.3, 157.2, 135.5, 132.0, 129.3 (2 C), 129.1 (2 C), 128.7 (2 C), 128.5 (2 C), 128.4 (2 C), 127.2, 123.3, 66.1, 60.6, 52.0, 51.6, 42.1, 40.9, 14.4, 12.9.

## Radioligand Binding Assays

Liver homogenates for S1R and S2R receptor binding assays were prepared from Sprague Dawley rats (ENVIGO RMS S.R.L., Udine, Italy). Radioligands [ $^3H$ ]-(+)-pentazocine (26.9 Ci/mmol) and [ $^3H$ ]DTG (35.5 Ci/mmol) were obtained from PerkinElmer (Zaventem, Belgium). Test compounds were dissolved in DMSO to create 10 mM stock solutions and diluted to final concentrations ( $10^{-5}$  M to  $10^{-11}$  M) using assay buffer.

For S1R assays, rat livers were homogenized in ice-cold buffer (0.32 M sucrose, pH 7.4), centrifuged twice, and the pellet resuspended in buffer with sucrose, EGTA,  $MgSO_4$ , and protease inhibitors. Protein concentration was determined using Bradford's method. Similarly, S2R assays involved liver homogenization in sucrose, followed by centrifugation and resuspension in ice-cold Tris buffer. *In vitro* S1R binding assays employed 250  $\mu g$  of rat livers membranes incubated with [ $^3H$ ]-(+)-pentazocine (2 nM) in Tris buffer (pH 8.0) for 150 min at 37 °C. Unlabeled (+)-pentazocine (10  $\mu M$ ) measured non-specific binding, and radioligand separation was done by filtration followed by scintillation counting. The  $K_d$  for

[ $^3H$ ]-(+)-pentazocine was 2.9 nM. For S2R assays, rat liver membranes (250  $\mu g$ ) were incubated with [ $^3H$ ]DTG (2 nM) and an S1R masking agent [(+)-pentazocine, 5  $\mu M$ ] for 120 min at rt. Non-specific binding was assessed with unlabeled DTG (10  $\mu M$ ), and radioligand was separated similarly. The  $K_d$  for [ $^3H$ ]DTG was 17.9 nM.  $K_i$  values were calculated using GraphPad Prism® 7.0 and reported as mean  $\pm$  SD from at least two independent experiments performed in duplicate.

## Molecular Modeling Studies

### Ligand Structures Preparation and Minimization

The molecular structures for all ligands used in this study were generated using Marvin Sketch (18.24, ChemAxon Ltd.). The 3D conformations were optimized using the PM6-D3H4 Hamiltonian implemented in the openMOPAC package (MOPAC v. 22.1.1, Stewart Computational Chemistry, Colorado Springs).<sup>[37]</sup>

Co-crystallized ligands, including PD144418, Z4857158944, and haloperidol, contain nitrogen atoms that are protonated at physiological pH (7.4), and their optimized structures reflect this as ammonium ions.

For compounds **17** and **19**, however, the presence of a fused pyrazole ring significantly lowers the basicity of the pyrrolidine nitrogen (calculated  $pK_a=5.39$  for 2,5-dimethyl-2H,4H,5H,6H-pyrrolo[3,4-c]pyrazole using Marvin Sketch).

Compounds **17**, which include an ester or amide substituent on the pyrrolidine nitrogen, exhibit an even lower basicity ( $pK_a=3.08$  for **17a**, calculated with Marvin Sketch). Conversely, compound **19** shows a calculated  $pK_a$  of 5.19. Notably, when a negatively charged residue (e.g., Glu or Asp) is near the ligand, the pyrrolidine nitrogen's  $pK_a$  is predicted to increase by approximately five units.<sup>[29]</sup> This suggests that compound **19**'s pyrrolidine nitrogen is likely protonated in the binding pocket and could form a stabilizing salt bridge with the Glu or Asp residue. So, all ligands were modeled in their protonated and deprotonated forms to validate this hypothesis. All stereoisomers were considered, including variations from protonating the pyrrolidine nitrogen. These stereoisomers are designated as ( $R/S_C/R/S_N$ ), where subscripts C and N refer to the stereochemistry of the carbon and nitrogen centers, respectively.

### S1R and S2R Structures Preparation

The crystal structures of human S1R bound to PD144418 (PDB ID: 5HK1) and bovine S2R complexed with Z4857158944 (PDB ID: 7M96) were retrieved from the PDB REDO database (<https://pdb-redo.eu/>). To model the human S2R, the bovine structure was used as a template, and the Homo sapiens S2R sequence (UniProt entry Q5BJF2) was applied as the target sequence using the YASARA Structure suite (v. 24.10.5, Biosciences GmbH, Vienna, Austria).<sup>[38]</sup> The quality of the obtained human S2R model was evaluated using Ramachandran plots via the PROCHECK server. Approximately 96.1% of residues were in the most favorable regions, 3.9% in allowed regions, and none in the disallowed regions, meeting the benchmark of > 90% for high-quality models (Figure S16). Further validation using the ERRAT server for non-bonded atomic interactions yielded an overall quality factor of 100 (Figure S17), affirming the model's reliability.

## Docking studies

Flexible docking simulations were performed using AutoDock Vina (v. 1.2.5) integrated within the YASARA Structure suite.<sup>[39]</sup> The simulation cell was defined with boundaries extending 5 Å from the ligand surface, following the protocol reported in the literature. Point charges were initially assigned according to the AMBER03 force field,<sup>[40]</sup> and then damped to mimic the less polar Gasteiger charges used to optimize the AutoDock scoring function. Default parameters were used for all other settings. The setup was done with the YASARA molecular modeling program and each ligand underwent 100 independent docking runs using the “dock\_runscreening” macro implemented in YASARA.

The free energy of binding ( $\Delta G$ ) associated with the top-ranked pose, as calculated by AutoDock Vina, was utilized to assess the affinity of each ligand. Subsequently, the  $\Delta G$  value was converted to the corresponding dissociation constant ( $K_d$ ) using the thermodynamic relationship:

$$K_d = e^{(\Delta G/RT)} \quad (1)$$

where the equation was evaluated at a temperature ( $T$ ) of 298.15 K and a gas constant ( $R$ ) of 0.0019872036 kcal/(K×mol).

## Author Contributions

Giuseppe Cosentino: Investigation, writing – original draft, writing – review and editing. Maria Dichiarà: Conceptualization, methodology, investigation, supervision, writing – original draft, writing – review & editing, data curation. Giuliana Costanzo: Investigation. Alessandro Coco: Investigation. Lorella Pasquucci: Writing – review and editing, supervision. Agostino Marrazzo: Writing – review and editing, supervision, funding acquisition. Antonio Rescifina: Methodology, writing – original draft, writing – review and editing supervision, data curation. Emanuele Amata: Conceptualization, methodology, supervision, funding acquisition, writing – original draft, writing – review & editing, data curation.

## Acknowledgements

This research was funded by Italian Minister of University and Research projects PRIN 2017–201744BN5T and PRIN 2022–P20224L3NK; European Cooperation in Science and Technology (COST) CA23156 – European Network for Sigma-1 Receptor as a Therapeutic Opportunity. Free academic license from ChemAxon for their suite of programs is gratefully acknowledged. Open Access publishing facilitated by Università degli Studi di Catania, as part of the Wiley - CRUI-CARE agreement.

## Conflict of Interests

There are no conflicts of interest to declare.

## Data Availability Statement

The data supporting this article have been included as part of the Supplementary Information.

**Keywords:** Medicinal chemistry · Molecular modeling · hERG inhibition · Sigma-1 receptor · Tetrahydropyrrolo[3,4-c]pyrazole.

- [1] a) J. Pergolizzi, G. Varrassi, *Cureus* **2023**, *15*, e42626; b) G. D. Walby, Q. Gu, H. Yang, S. F. Martin, *Bioorg. Chem.* **2024**, *145*, 107191; c) J. Pergolizzi, G. Varrassi, M. Coleman, F. Breve, D. K. Christo, P. J. Christo, C. Moussa, *Cureus* **2023**, *15*, e35756; d) N. T. Nguyen, V. Jaramillo-Martinez, M. Mathew, V. V. Suresh, S. Sivaprakasam, Y. D. Bhutia, V. Ganapathy, *International J. Mol. Sci.* **2023**, *24*; e) F. S. Abatematteo, M. Niso, E. Lacivita, C. Abate, *Molecules* **2021**, *26*, 3743.
- [2] a) H. R. Schmidt, S. Zheng, E. Gurpinar, A. Koehl, A. Manglik, A. C. Kruse, *Nature* **2016**, *532*, 527–530; b) D. S. Malar, P. Thitilertdech, K. S. Ruckvongacheep, S. Brimson, T. Tencomnao, J. M. Brimson, *CNS Drugs* **2023**, *37*, 399–440.
- [3] S. Couly, N. Gogvadze, Y. Yasui, Y. Kimura, S. M. Wang, N. Sharikadze, H. E. Wu, T. P. Su, *Cellular and Molecular Neurobiol.* **2022**, *42*, 597–620.
- [4] a) V. Lachance, S. M. Bélanger, C. Hay, V. Le Corvec, V. Banouvong, M. Lapalme, K. Tarmoun, G. Beaucaire, M. P. Lussier, S. Kourrich, *Int. J. Mol. Sci.* **2023**, *24*, 1971; b) D. A. Ryskamp, S. Korban, V. Zhemkov, N. Kraskovskaya, I. Bezprozvanny, *Front. Neurobiol.* **2019**, *13*, 862.
- [5] a) P. Ren, J. Wang, N. Li, G. Li, H. Ma, Y. Zhao, Y. Li, *Frontiers Pharmacol.* **2022**, *13*, 925879; b) K. Yang, C. Wang, T. Sun, *Frontiers Pharmacol.* **2019**, *10*, 528; c) L. Romero, M. Merlos, J. M. Vela, *Advances in Pharmacol. (San Diego, Calif.)* **2016**, *75*, 179–215; d) E. Arena, M. Dichiarà, G. Floresta, C. Parenti, A. Marrazzo, V. Pittalà, E. Amata, O. Prezzavento, *Future Medicinal Chem.* **2018**, *10*, 231–256.
- [6] a) Y. Lu, Q. Gu, S. F. Martin, *Euro. J. Med. Chem.* **2023**, *257*, 115488; b) G. D. Walby, Q. Gu, H. Yang, S. F. Martin, *Bioorganic Chem.* **2024**, *145*, 107191; c) H. M. Oyer, C. M. Sanders, F. J. Kim, *Front. Pharmacol.* **2019**, *10*, 1141.
- [7] a) E. Vázquez-Rosa, M. R. Watson, J. J. Sahn, T. R. Hodges, R. E. Schroeder, C. J. Cintrón-Pérez, M. K. Shin, T. C. Yin, J. L. Emery, S. F. Martin, D. J. Liebl, A. A. Pieper, *ACS Chem. Neurosci.* **2019**, *10*, 1595–1602; b) B. Yi, J. J. Sahn, P. M. Ardestani, A. K. Evans, L. L. Scott, J. Z. Chan, S. Iyer, A. Crisp, G. Zuniga, J. T. Pierce, S. F. Martin, M. Shamloo, *J. Neurochem.* **2017**, *140*, 561–575.
- [8] a) A. Piechal, A. Jakimiuk, D. Mirowska-Guzel, *Pharmacological Reports : PR* **2021**, *73*, 1582–1594; b) R. S. E. Keefe, P. D. Harvey, A. Khan, J. B. Saoud, C. Stamer, M. Davidson, R. Luthringer, *J. Clinical Psych.* **2018**, *79*, 17m11753.
- [9] a) F. Weber, B. Wünsch, *Handbook of Experimental Pharmacol.* **2017**, *244*, 51–79; b) F. Meng, Y. Xiao, Y. Ji, Z. Sun, X. Zhou, *Nat. Commun.* **2022**, *13*, 1267.
- [10] K. Szczepańska, S. Podlewska, M. Dichiarà, D. Gentile, V. Patamia, N. Rosier, D. Mönnich, M. C. Ruiz Cantero, T. Karcz, D. Łażewska, A. Siwek, S. Pockes, E. J. Cobos, A. Marrazzo, H. Stark, A. Rescifina, A. J. Bojarski, E. Amata, K. Kieć-Kononowicz, *ACS Chem. Neurosci.* **2022**, *13*, 1–15.
- [11] G. Costanzo, G. Cosentino, L. Pasquucci, E. Amata, D. Schepmann, B. Wünsch, *ChemMedChem* **2024**, *19*, e202400596.
- [12] M. Dichiarà, F. A. Ambrosio, S. M. Lee, M. C. Ruiz-Cantero, J. Lombino, A. Coricello, G. Costa, D. Shah, G. Costanzo, L. Pasquucci, K. N. Son, G. Cosentino, R. González-Cano, A. Marrazzo, V. K. Aakalu, E. J. Cobos, S. Alcaro, E. Amata, *J. Med. Chem.* **2023**, *66*, 11447–11463.
- [13] a) Z. Fan, Y. Xiao, Y. Shi, C. Hao, Y. Chen, G. Zhang, T. Zhuang, X. Cao, *Biochem. Biophys. Res. Commun.* **2024**, *697*, 149547; b) T. Conroy, M. Manohar, Y. Gong, S. M. Wilkinson, M. Webster, B. P. Lieberman, S. D. Banister, T. A. Reekie, R. H. Mach, L. M. Rendina, M. Kassiou, *Organic Biomol. Chem.* **2016**, *14*, 9388–9405.
- [14] a) K. Sałaciak, K. Pytka, *Neuroscience Biobehavioral Rev.* **2022**, *132*, 1114–1136; b) T. Maurice, *Behavioural Brain Res.* **2016**, *296*, 270–278; c) M. Page, N. Pacico, S. Ourtioualou, T. Deprez, K. Koshibu, *Pharmacology* **2015**, *96*, 131–136; d) T. Niitsu, M. Iyo, K. Hashimoto, *Current Pharma. Design* **2012**, *18*, 875–883; e) R. Urfer, H. J. Moebius, D. Skoloudik, E. Santamarina, W. Sato, S. Mita, K. W. Muir, *Stroke* **2014**, *45*, 3304–3310; f) N. Ye, W. Qin, S. Tian, Q. Xu, E. A. Wold, J. Zhou, X. C. Zhen, *J. Med. Chem.* **2020**, *63*, 15187–15217.
- [15] Y. Peng, Q. Zhang, W. J. Welsh, *J. Med. Chem.* **2021**, *64*, 890–904.

- [16] U. Christmann, L. Garriga, A. V. Llorente, J. L. Díaz, R. Pascual, M. Bordas, A. Dordal, M. Porras, S. Yeste, R. F. Reinoso, J. M. Vela, C. Almansa, *J. Med. Chem.* **2024**, *67*, 9150–9164.
- [17] a) G. Lin, Q. Xu, J. Li, Z. Chu, X. Ma, Q. Zhu, Y. Zhao, J. Mo, W. Ye, L. Shao, T. Fang, M. He, S. Yue, M. Dai, *J. Med. Chem.* **2024**, *67*, 3358–3384; b) L. Gebauer, O. Jensen, M. Rafahi, J. Brockmüller, *J. Med. Chem.* **2023**, *66*, 15990–16001; c) J. Xiong, T. Zhuang, Y. Ma, J. Xu, J. Ye, R. Ma, S. Zhang, X. Liu, B. F. Liu, C. Hao, G. Zhang, Y. Chen, *Euro J Medicinal Chem.* **2021**, *226*, 113879.
- [18] L. A. Nguyen, H. He, C. Pham-Huy, *Int. J Biomed. Sci.: IJBS* **2006**, *2*, 85–100.
- [19] O. Prezzavento, E. Arena, C. Sánchez-Fernández, R. Turnaturi, C. Parenti, A. Marrazzo, R. Catalano, E. Amata, L. Pasquinucci, E. J. Cobos, *European J Med. Chem.* **2017**, *125*, 603–610.
- [20] J. Köhler, K. Bergander, J. Fabian, D. Schepmann, B. Wünsch, *J. Med. Chem.* **2012**, *55*, 8953–8957.
- [21] D. Fancelli, J. Moll, M. Varasi, R. Bravo, R. Artico, D. Berta, S. Bindi, A. Cameron, I. Candiani, P. Cappella, P. Carpinelli, W. Croci, B. Forte, M. L. Giorgini, J. Klapwijk, A. Marsiglio, E. Pesenti, M. Rocchetti, F. Roletto, D. Severino, C. Soncini, P. Storici, R. Tonani, P. Zugnoni, P. Vianello, *J. Med. Chem.* **2006**, *49*, 7247–7251.
- [22] H. R. Schmidt, R. M. Betz, R. O. Dror, A. C. Kruse, *Nature Struct. Mol. Biol.* **2018**, *25*, 981–987.
- [23] a) S. Su, J. Sun, Y. Wang, Y. Xu, *Handb. Exp. Pharmacol.* **2021**, *267*, 139–166; b) Y. Wang, Y. Liu, Y. Zhang, Z. Zhang, L. Xu, J. Wang, Y. Yang, B. Hu, Y. Yao, M. Wei, J. Wang, B. Tang, K. Zhang, S. Liu, G. Yang, *Euro. J Medicinal Chem.* **2024**, *271*, 116395; c) J. R. Hummel, K. J. Xiao, J. C. Yang, L. B. Epling, K. Mukai, Q. Ye, M. Xu, D. Qian, L. Huo, M. Weber, V. Roman, Y. Lo, K. Drake, K. Stump, M. Covington, K. Kapilashrami, G. Zhang, M. Ye, S. Diamond, S. Yeleswaram, R. Macarron, M. C. Deller, S. Wee, S. Kim, X. Wang, L. Wu, W. Yao, *J. Med. Chem.* **2024**, *67*, 3112–3126; d) G. Thoma, C. Markert, R. Lueoend, W. Miltz, C. Spanka, B. Bollbuck, R. M. Wolf, H. Srinivas, C. A. Penno, M. Kiffe, M. Gajewska, D. Bednarczyk, G. Wiczorek, A. Evans, C. Beerli, T. A. Röhn, *J. Med. Chem.* **2023**, *66*, 16410–16425; e) Z. Li, X. Wang, Y. Lin, Y. Wang, S. Wu, K. Xia, C. Xu, H. Ma, J. Zheng, L. Luo, F. Zhu, S. He, X. Zhang, *Euro. J Medicinal Chem.* **2020**, *205*, 112537; f) T. Biftu, R. Sinha-Roy, P. Chen, X. Qian, D. Feng, J. T. Kuethe, G. Scapin, Y. D. Gao, Y. Yan, D. Krueger, A. Bak, G. Eiermann, J. He, J. Cox, J. Hicks, K. Lyons, H. He, G. Salituro, S. Tong, S. Patel, G. Doss, A. Petrov, J. Wu, S. S. Xu, C. Sewall, X. Zhang, B. Zhang, N. A. Thornberry, A. E. Weber, *J. Med. Chem.* **2014**, *57*, 3205–3212.
- [24] J. L. Diaz, F. Cuevas, A. I. Oliva, D. Font, M. Sarmentero, P. Álvarez-Bercedo, J. M. López-Valbuena, M. A. Pericàs, R. Enrech, A. Montero, S. Yeste, A. Vidal-Torres, I. Álvarez, P. Pérez, C. M. Cendán, E. J. Cobos, J. M. Vela, C. Almansa, *J. Med. Chem.* **2021**, *64*, 5157–5170.
- [25] E. Badiola, B. Fiser, E. Gómez-Bengoia, A. Mielgo, I. Olaizola, I. Urruzuno, J. M. García, J. M. Odriozola, J. Razkin, M. Oiarbide, C. Palomo, *J. Am. Chem. Soc.* **2014**, *136*, 17869–17881.
- [26] a) A. Jones, M. I. Kemp, M. L. Stockley, M. D. Woodrow, in *World Intellectual Property Organization, Patent No. WO 2017/158381* **2017**; b) K. W. Bair, Baumeister, R. Timm, Dragoyich, Peter, Gosslein, Francis Yuen, Po-Wai, Zak, Mark, *WO2013/127267* **2013**.
- [27] K. N. Vijayadas, R. V. Nair, R. L. Gawade, A. S. Kotmale, P. Prabhakaran, R. G. Gonnade, V. G. Puranik, P. R. Rajamohanam, G. J. Sanjayan, *Org. Biomol. Chem.* **2013**, *11*, 8348–8356.
- [28] A. Cavalli, E. Poluzzi, F. De Ponti, M. Recanatini, *J. Med. Chem.* **2002**, *45*, 3844–3853.
- [29] H. Yano, A. Bonifazi, M. Xu, D. A. Guthrie, S. N. Schneck, A. M. Abramyan, A. D. Fant, W. C. Hong, A. H. Newman, L. Shi, *Neuropharmacology* **2018**, *133*, 264–275.
- [30] A. Alon, J. Lyu, J. M. Braz, T. A. Tummino, V. Craik, M. J. O'Meara, C. M. Webb, D. S. Radchenko, Y. S. Moroz, X. P. Huang, Y. Liu, B. L. Roth, J. J. Irwin, A. I. Basbaum, B. K. Shoichet, A. C. Kruse, *Nature* **2021**, *600*, 759–764.
- [31] a) V. Mégalizzi, V. Mathieu, T. Mijatovic, P. Gailly, O. Debeir, N. De Neve, M. Van Damme, G. Bontempi, B. Haibe-Kains, C. Decaestecker, Y. Kondo, R. Kiss, F. Lefranc, *Neoplasia (New York, N. Y.)* **2007**, *9*, 358–369; b) M. P. Davis, *Expert Opin. Drug Discovery* **2015**, *10*, 885–900; c) G. Gris, E. Portillo-Salido, B. Aubel, Y. Darbaky, K. Deseure, J. M. Vela, M. Merlos, D. Zamanillo, *Sci. Rep.* **2016**, *6*, 24591.
- [32] W. Fischl, C. J. Yarnold, P. L. Amouzegh, K. Thewlis, J. Shepherd, M. A. Kerry, in *U.S. Patent and Trademark Office, Patent No. 11,180,479 B2* **2021**.
- [33] a) H. Liu, S. Ueta, F. Yagishita, M. Nishiuchi, Y. Kawamura, *Tetrahedron* **2015**, *71*, 3614–3618; b) H. Prydderch, A. Haiß, M. Spulak, B. Quilty, K. Kümmerer, A. Heise, N. Gathergood, *RSC Adv.* **2017**, *7*, 2115–2126; c) K. Ohno, Y. Ma, Y. Huang, C. Mori, Y. Yahata, Y. Tsujii, T. Maschmeyer, J. Moraes, S. Perrier, *Macromolecules* **2011**, *44*, 8944–8953; d) X. Zhang, J. Lin, M. C. Liu, Y. B. Zhou, H. Y. Wu, *Euro. J Org Chem.* **2024**, *27*, e202300958.
- [34] P. S. Lai, J. A. Dubland, M. G. Sarwar, M. G. Chudzinski, M. S. Taylor, *Tetrahedron* **2011**, *67*, 7586–7592.
- [35] a) A. Jones, M. I. Kemp, M. L. Stockley, M. D. Woodrow, in *World Intellectual Property Organization, Patent No. WO 2017/158381* **2017**; b) A. I. Frolov, E. N. Ostapchuk, A. E. Pashenko, Y. O. Chuchvera, E. B. Rusanov, D. M. Volochnyuk, S. V. Ryabukhin, *J. Org. Chem.* **2021**, *86*, 7333–7346; c) D. N. Deaton, C. D. Haffner, B. R. Henke, M. R. Jeune, B. G. Shearer, E. L. Stewart, J. D. Stuart, J. C. Ulrich, *Bioorg. Med. Chem.* **2018**, *26*, 2107–2150.
- [36] V. J. Santora, T. A. Almos, R. Barido, J. Basinger, C. L. Bellows, B. C. Bookser, J. G. Breitenbucher, N. J. Broadbent, C. Cabebe, C. K. Chai, M. Chen, S. Chow, D. M. Chung, L. Crickard, A. M. Danks, G. C. Freestone, D. Gitnick, V. Gupta, C. Hoffmaster, A. R. Hudson, A. P. Kaplan, M. R. Kennedy, D. Lee, J. Limberis, K. Ly, C. C. Mak, B. Masatsugu, A. C. Morse, J. Na, D. Neul, J. Nikpur, M. Peters, R. E. Petroski, J. Renick, K. Sebring, S. Sevidal, A. Tabatabaei, J. Wen, Y. Yan, Z. W. Yoder, D. Zook, *J. Med. Chem.* **2018**, *61*, 6018–6033.
- [37] J. Řezáč, P. Hobza, *J Chemical Theory Comput.* **2012**, *8*, 141–151.
- [38] K. Ozvoldik, T. Stockner, E. Krieger, *J. Chem. Inf. Model.* **2023**, *63*, 6177–6182.
- [39] J. Eberhardt, D. Santos-Martins, A. F. Tillack, S. Forli, *J. Chem. Inf. Model.* **2021**, *61*, 3891–3898.
- [40] Y. Duan, C. Wu, S. Chowdhury, M. C. Lee, G. Xiong, W. Zhang, R. Yang, P. Cieplak, R. Luo, T. Lee, J. Caldwell, J. Wang, P. Kollman, *J Comput. hemistry* **2003**, *24*, 1999–2012.

Manuscript received: December 18, 2024

Revised manuscript received: January 21, 2025

Accepted manuscript online: January 30, 2025

Version of record online: February 9, 2025